Two-proton radioactivity of ground and excited states within a unified fission model*

Fengzhu Xing(邢凤竹)[1,2] Jianpo Cui(崔建坡)[1,2] Yanzhao Wang(王艳召)[1,2,3†] Jianzhong Gu(顾建中)[3‡]

[1]Department of Mathematics and Physics, Shijiazhuang Tiedao University, Shijiazhuang 050043, China
[2]Institute of Applied Physics, Shijiazhuang Tiedao University, Shijiazhuang 050043, China
[3]China Institute of Atomic Energy, P. O. Box 275 (10), Beijing 102413, China

Abstract: A unified fission model is extended to study two-proton radioactivity of the ground states of nuclei, and a good agreement between the experimental and calculated half-lives is found. The two-proton radioactivity half-lives of the ground states of some probable candidates are predicted within this model by inputting the released energies taken from the AME2020 table. It is shown that the predictive accuracy of the half-lives is comparable to those of other models. Then, two-proton radioactivity of the excited states of ^{14}O, ^{17,18}Ne, ^{22}Mg, ^{29}S, and ^{94}Ag is discussed within the unified fission model and two analytical formulas. It is found that the experimental half-lives of the excited states are reproduced better within the unified fission model. Furthermore, the two formulas are not suitable for the study of two-proton radioactivity of excited states because their physical appearance deviates from the mechanism of quantum tunneling, and the parameters involved are obtained without including experimental data from the excited states.

Keywords: two-proton radioactivity, released energy, half-life, unified fission model, analytical formula

DOI: 10.1088/1674-1137/ac2425

I. INTRODUCTION

Two-proton ($2p$) radioactivity is an exotic decay mode with an emission of two protons from the nuclei near the $2p$ drip-line. In 1960, Zel'dovich predicted the possibility that a pair of protons might be emitted from the ground state of a nucleus [1], a phenomenon that was named "$2p$ radioactivity" by Goldansky [2, 3]. Due to the proton pairing effect, $2p$ radioactivity usually occurs in the even-Z nuclei so that one-proton ($1p$) radioactivity is strongly forbidden or substantially suppressed. Moreover, during the process of $2p$ emission, the energy level of the $2p$ emitting channel is lower than that of $1p$ radioactivity. $2p$ emission is called true $2p$ radioactivity and has $Q_{2p} > 0$ and $Q_p < 0$ (Q_{2p} and Q_p are the released energies of $2p$ and $1p$ radioactivity, respectively). [4-6]. Although some probable $2p$ radioactivity candidates, such as ^{39}Ti, ^{42}Cr, ^{45}Fe, and ^{48,49}Ni, were predicted by various models [2, 3, 7-13], $2p$ radioactivity had not been discovered for a long time. More than 40 years later, ground-state true $2p$ radioactivity was observed for the first time from ^{45}Fe [14, 15] and then from the ground states of ^{54}Zn [16], ^{48}Ni [17], and ^{67}Kr [18]. So far, ground state $2p$ radioactivity with long half-lives has only been observed from those four nuclides. In addition, extremely short-lived $2p$ radioactivity from the ground state was observed from ^{6}Be [19], ^{12}O [20-23], ^{16}Ne [21, 24], and ^{19}Mg [25]. For ^{6}Be, ^{12}O, and ^{16}Ne, the decaying states have large widths so that the $2p$ emitter states and the $1p$ daughter states overlap with each other. Therefore, the decay will most likely take place sequentially [4-6, 26]. However, the situation of ^{19}Mg is less clear because the structure and mass of ^{18}Na (its $1p$ daughter nucleus) are experimentally unobtainable. The wave function is more confined in the nuclear interior because of its stronger Coulomb barrier, which causes the narrower decay states.

In addition to ground state $2p$ radioactivity,$2p$ emission may take place from the excited states. In 1980, Goldansky predicted that β-delayed $2p$ ($\beta 2p$) radioactivity candidates could be found in the $\beta 2p$ emitters of Z = 10~20 [27]. Shortly after that, the $\beta 2p$ radioactivity of ^{22}Al was observed for the first time in the Lawrence

Received 10 July 2021; Accepted 7 September 2021; Published online 15 October 2021

* Supported by the National Natural Science Foundation of China (U1832120, 11675265), the Natural Science Foundation for Outstanding Young Scholars of Hebei Province of China (A2020210012, A2018210146), the Natural Science Foundation of Hebei Province of China (A2021210010), the Continuous Basic Scientific Research Project (WDJC-2019-13) and the Leading Innovation Project (LC 192209000701)

† E-mail: yanzhaowang09@126.com
‡ E-mail: jzgu1963@ciae.ac.cn

Berkeley National Laboratory [28]; subsequently, more $\beta 2p$ nuclei, such as ^{23}Si [29], ^{26}P [30], ^{27}S [31], ^{31}Ar [32], ^{35}Ca [33], ^{39}Ti [34], ^{43}Cr [35, 36], and ^{50}Ni [37] were discovered. In addition to populating excited $2p$ emitter states with β decays, some $2p$ emitters (^{14}O [38], ^{17,18}Ne [39-43], ^{22}Mg [44, 45], and ^{28,29}S [46, 47]) were discovered from the excited states fed by nuclear reactions such as pick up, transfer, and fragmentation reactions. Recently, the $2p$-radioactive decay from an abnormal, spinning, and long-lived state of ^{94}Ag was reported for the first time by Mukha *et al.* [48].

To understand the mechanism of $2p$ radioactivity, several microscopic and phenomenological models have been proposed [10, 11, 49-73]. Generally, the mechanisms are divided into the following three types [5, 6]: (i) ^{2}He cluster emission, (ii) three-body emission, and (iii) sequential emission. In ^{2}He cluster emission, the two protons are strongly correlated and constitute a quasi-bound $^1S_0$ configuration with a very short lifetime. Then, such a quasi-bound state becomes separated after penetrating the Coulomb barrier. For three-body emission, the nuclear core and the two protons separate simultaneously, and the two protons are only relevant to the final correlation and are emitted from the parent nucleus. For sequential emission, the initial nucleus first decays to an intermediate state via the emission of a proton; by subsequently emitting the other proton from the intermediate state, the final state is formed. Hence, sequential emission can be seen as twice $1p$ sequential emission. Because the nucleon wave function configurations and the nucleon-nucleon interaction are involved in the two correlated protons, the first two mechanisms attract the interests of researchers. Furthermore, the study of $2p$ radioactivity is significant for nuclear astrophysics. For example, $2p$ radioactivity is highly relevant to the $(2p,\gamma)$ and $(\gamma, 2p)$ processes of stellar evolution, which are important for studying the nuclear characteristics at waiting-points [74]. Thus, studies on the structures and properties of the $2p$ radioactivity nuclei become an important frontier in modern nuclear physics.

It is well known that $1p$, α, and cluster radioactivity are important decay modes for unstable nuclei. These emissions can be regarded as super-asymmetric quasi-fission processes of nuclei; therefore, they can be described by a universal approach based on nuclear fission theory. The unified fission model (UFM) can accurately predict the half-lives of these types of radioactivity [75-81]. From this, we consider whether $2p$ radioactivity can be studied and described by the UFM if the two emitted protons are seen as a ^{2}He cluster. Therefore, it is interesting to extend the UFM to study $2p$ radioactivity. This constitutes the motivation of our article, which is organized as follows. In Sec. II, the theoretical framework of the UFM is introduced. In Sec. III, the calculated results and relevant discussions are presented. In the last section, the conclusions are summarized.

II. UFM

In this study, the UFM we used is a modified version of the preformed cluster model proposed by Gupta and collaborators [75-77]. In the framework of the UFM, the $2p$-pair with zero binding energy is preformed near the nuclear surface and separates quickly due to the dominance of the Coulomb repulsion after escaping from the barrier.

The half-life is expressed as

$$T_{2p} = \frac{\ln 2}{S_{2p}\nu_0 P}, \tag{1}$$

where S_{2p} is the preformation factor of the ^{2}He cluster, which is similar to the preformation factor of an α-particle in the α-decay process or the spectroscopic factor of $1p$ radioactivity. It can be estimated using the cluster overlap approximation [11]

$$S_{2p} = G^2[A_0/(A_0-2)]^{2n}\chi^2. \tag{2}$$

Here, $G^2 = (2n)!/[2^{2n}(n!)^2]$ [82], and n is the average principal proton oscillator quantum number given by $n \approx (3Z_0)^{1/3} - 1$ [83]. A_0 and Z_0 are the mass number and charge number of the parent nucleus, respectively. χ^2 is the proton overlap function, which is determined by fitting the experimental Q_{2p} values and half-lives [57]. ν_0 is the assault frequency of the $2p$-pair on the barrier of the parent nucleus and is estimated by the following classical method:

$$\nu_0 = \frac{1}{2R_0}\sqrt{\frac{2E_{2p}}{M_{2p}}}, \tag{3}$$

where R_0 is the radius of the parent nucleus. E_{2p} and M_{2p} represent the kinetic energy and the mass of the emitted $2p$-pair, respectively.

The penetrability P is calculated by the WKB approximation, which is expressed as

$$P = \exp\left[-\frac{2}{\hbar}\int_{R_{\rm in}}^{R_{\rm out}}\sqrt{2\mu(V(r)-Q_{2p})}{\rm d}r\right], \tag{4}$$

where $R_{\rm in}$ and $R_{\rm out}$ are the first and second turning points, respectively, with $V(R_{\rm in}) = V(R_{\rm out}) = Q_{2p}$. μ is the reduced mass of the $2p$-pair and the residual daughter nucleus. The potential $V(r)$ is parameterized simply as a polynomial for $r \leqslant R_1 + R_2$, which is expressed as

$$V(r) = a_0 + a_1 r + a_2 r^2, \tag{5}$$

where the coefficients a_0, a_1, and a_2 are determined by the following boundary conditions:

(i) At $r = R_0 = R_{in}$, $V(r) = Q_{2p}$;

(ii) At $r = R_1 + R_2$, $V(r) = V(R_1 + R_2)$;

(iii) At $r = R_1 + R_2$, $V'(r) = V'(R_1 + R_2)$.

Here, R_1 and R_2 are the radii of the daughter nucleus and the emitted cluster, respectively. The radii measured in fm are given by

$$R_i = (1.28A_i^{1/3} - 0.76 + 0.8A_i^{-1/3}), i = 0, 1, 2. \tag{6}$$

However, for $r \geqslant R_1 + R_2$, $V(r)$ is composed of the repulsive Coulomb potential, attractive proximity potential, and centrifugal potential and is written as

$$V(r) = V_p(r) + V_l(r) + \frac{Z_1 Z_2 e^2}{r}, \tag{7}$$

where Z_1 and Z_2 are the charge numbers of the emitted particle and daughter nucleus, respectively.

V_p is an additional attraction due to the nuclear proximity potential, whose form can be found in Refs. [76, 77, 79-81]. The centrifugal potential $V_l(r)$ due to the angular momentum of the emitted $2p$-pair (l) takes the following form:

$$V_l(r) = \frac{l(l+1)\hbar^2}{2\mu r^2}. \tag{8}$$

III. RESULTS AND DISCUSSIONS

The $2p$ radioactivity half-lives of the ground-state to ground-state transitions are calculated within the UFM by inputting the experimental Q_{2p} values. In Table 1, column 1 contains the $2p$ emitters, and column 2 shows the experimental Q_{2p} values. From calculations, the adjustable parameter χ^2 is determined as 0.038 by fitting the experimental Q_{2p} values and half-lives; hence, the S_{2p} values can be obtained using Eq. (2), which are shown in column 3. The experimental and the calculated logarithm half-lives within the UFM, the generalized liquid drop model (GLDM) [57], the effective liquid drop model (ELDM) [58], and the Gomow-like model [59] are listed in the 4th-8th columns. The error bars of the calcu-

Table 1. Comparison between the experimental $2p$ radioactivity half-lives of the ground states and those within different models. The $Q_{2p}^{\rm expt.}$ and $\log_{10}T_{1/2}$ values are measured in MeV and s, respectively.

Nuclei	$Q_{2p}^{\rm expt.}$/MeV	S_{2p}	$\log_{10}T_{1/2}^{\rm 2p}$/s					$\log_{10}HF$
			Expt.	UFM	GLDM [57]	ELDM [58]	Gamow-like [59]	UFM
$^{6}_{4}$Be	1.371(5) [19]	0.043	$-20.30^{+0.03}_{-0.03}$ [19]	$-19.41^{+0.003}_{-0.003}$	$-19.37^{+0.01}_{-0.01}$	−19.97	−19.70	−0.89
$^{12}_{8}$O	1.638(24) [20]	0.030	>−20.20 [20]	$-18.45^{+0.04}_{-0.03}$	$-19.17^{+0.13}_{-0.08}$	−18.27	−18.04	>−1.75
	1.820(120) [21]	0.030	$-20.94^{+0.43}_{-0.21}$ [21]	$-18.69^{+0.15}_{-0.14}$	$-19.46^{+0.13}_{-0.07}$		−18.30	−2.25
	1.790(40) [22]	0.030	$-20.10^{+0.18}_{-0.13}$ [22]	$-18.65^{+0.05}_{-0.05}$	$-19.43^{+0.04}_{-0.03}$		−18.26	−1.45
	1.800(400) [23]	0.030	$-20.12^{+0.78}_{-0.26}$ [23]	$-18.66^{+0.62}_{-0.41}$	$-19.44^{+0.30}_{-0.20}$		−18.27	−1.46
$^{16}_{10}$Ne	1.330(80) [21]	0.024	$-20.64^{+0.30}_{-0.18}$ [21]	$-16.49^{+0.24}_{-0.22}$	$-16.45^{+0.23}_{-0.21}$		−16.23	−4.15
	1.400(20) [24]	0.024	$-20.38^{+0.20}_{-0.13}$ [24]	$-16.68^{+0.05}_{-0.05}$	$-16.63^{+0.05}_{-0.05}$	−16.60	−16.43	−3.70
$^{19}_{12}$Mg	0.750(50) [25]	0.022	$-11.40^{+0.14}_{-0.20}$ [25]	$-11.77^{+0.47}_{-0.43}$	$-11.79^{+0.47}_{-0.42}$	−11.72	−11.46	0.37
$^{45}_{26}$Fe	1.100(100) [14]	0.016	$-2.40^{+0.26}_{-0.26}$ [14]	$-1.94^{+1.34}_{-1.18}$	$-2.23^{+1.34}_{-1.17}$		−2.09	−0.46
	1.140(50) [15]	0.016	$-2.07^{+0.24}_{-0.21}$ [15]	$-2.43^{+0.61}_{-0.58}$	$-2.71^{+0.61}_{-0.57}$		−2.58	0.36
	1.154(16) [17]	0.016	$-2.55^{+0.13}_{-0.12}$ [17]	$-2.60^{+0.19}_{-0.18}$	$-2.87^{+0.19}_{-0.18}$	−2.43	−2.74	0.05
	1.210(50) [84]	0.016	$-2.42^{+0.03}_{-0.03}$ [84]	$-3.23^{+0.56}_{-0.52}$	$-3.50^{+0.56}_{-0.52}$		−3.37	0.81
$^{48}_{28}$Ni	1.290(40) [85]	0.015	$-2.52^{+0.24}_{-0.22}$ [85]	$-2.29^{+0.44}_{-0.41}$	$-2.62^{+0.44}_{-0.42}$		−2.59	−0.23
	1.350(20) [17]	0.015	$-2.08^{+0.40}_{-0.78}$ [17]	$-2.91^{+0.21}_{-0.19}$	$-3.24^{+0.20}_{-0.20}$		−3.21	0.83
	1.310(40) [86]	0.015	$-2.52^{+0.24}_{-0.22}$ [87]	$-2.50^{+0.43}_{-0.41}$	$-2.83^{+0.43}_{-0.41}$	−2.36	0.015	−0.02
$^{54}_{30}$Zn	1.280(210) [88]	0.015	$-2.76^{+0.15}_{-0.14}$ [88]	$-0.52^{+2.80}_{-2.18}$	$-0.87^{+0.25}_{-0.24}$		−0.93	−2.24
	1.480(20) [16]	0.015	$-2.43^{+0.20}_{-0.14}$ [16]	$-2.61^{+0.19}_{-0.19}$	$-2.95^{+0.19}_{-0.19}$	−2.52	−3.01	0.18
$^{67}_{36}$Kr	1.690(17) [18]	0.013	$-1.70^{+0.02}_{-0.02}$ [18]	$-0.54^{+0.16}_{-0.16}$	$-1.25^{+0.16}_{-0.16}$	−0.06	−0.76	−1.16

lated half-lives in columns 4 and 5 result from the errors of the experimental Q_{2p} values. Note that for $2p$ radioactivity of these nuclei, the l values are all zero. Therefore, the centrifugal potential contribution to the half-life vanishes. In order to analyze the deviation of the experimental half-lives from the calculated ones, the values of the logarithm hindrance factor $\log_{10}HF$ ($\log_{10}HF=\log_{10}T_{1/2}^{\rm expt.}-\log_{10}T_{1/2}^{\rm UFM}$) are listed in the final column of Table 1. From Table 1, an agreement between the calculated half-lives and the experimental data is found. Furthermore, it can be seen that the calculated half-lives within the UFM are similar to those within the three other models. Hence, the UFM can be considered to have a comparable accuracy to that of the other models.

Encouraged by the success of the UFM, we attempt to predict the half-lives of the most probable $2p$ decay candidates within it. In our recent study [89], we predicted the half-lives of the most probable $2p$ decay candidates within the GLDM by inputting the Q_{2p} values extracted from the mass tables of the Weizsäcker-Skyrme-4 model [90], the finite-range droplet model [91], the Koura-Tachibana-Uno-Yamada model [92], and the Hartree-Fock-Bogoliubov mean-field model with the BSk29 Skyrme interaction [93]. It was shown that the uncertainties of the $2p$ decay half-lives are rather large due to the strong model dependence of the Q_{2p} values; and therefore, accurate Q_{2p} values are crucial for predicting the $2p$ radioactive half-lives. Thus, the newest Q_{2p} values ($Q_{2p}\approx -S'_{2p}$, where S'_{2p} refers to the two-proton separation energy) from the AME2020 table [94] (See column 2 of Table 2) are used for predicting the $2p$ radioactive half-lives. The S_{2p} values given by Eq. (2) and the l values are shown in columns 3 and 4 of Table 2, respectively. Note that the l values are determined by the spin-parity selection rule, and the spin and parity values of the initial and final states are taken from the NUBASE2020 table [95]. The predicted $2p$ radioactive half-lives within the UFM are shown in column 5 of Table 2. In addition, the half-lives are predicted within the GLDM and ELDM with the methods used in Refs. [57-89], which are listed in the last two columns of Table 2. Table 2 shows that the majority of the half-lives within the different models are similar to one another. In these models, $2p$ radioactivity is treated as a process in which a ^{2}He cluster is first preformed on the nuclear surface and then penetrates the barrier between the ^{2}He cluster and the daughter nucleus. Thus, these models share the same mechanism which leads to similar half-lives. Since the mechanism of $2p$ radioactivity is similar to that of α-decay [96-100], the cluster-like or fission-like models that can describe α-decay can reproduce the experimental half-lives of $2p$ radioactivity. Recently, an extended constraint criterion on the half-life, $-12<\log_{10}T_{1/2}^{\rm 2p}<2$ s, was proposed to identify the most probable $2p$ decay candidates [89] for future experiments, based on the work of Olsen *et al.* [62]. According to the constraint condition, the most probable $2p$ decay candidates listed in Table 2 are ^{24}P, ^{39}Ti, ^{40}V, ^{42}Cr, ^{43}Mn, ^{47}Co, ^{49}Ni, ^{56,57}Ga, ^{58,59}Ge, ^{60,61}As, ^{63}Se, ^{65,66}Br, and ^{68}Kr.

In addition to the mentioned models, two analytical formulas that estimate the ground state $2p$ radioactivity half-lives were recently proposed by extending the empirical formulas for $1p$ radioactivity based on the Geiger-Nuttall law [60, 61], which are denoted as the formula of Sreeja and the formula of Liu in this article. Sreeja's formula is expressed as [60]

$$\log_{10}T_{1/2}=(al+b)\xi+cl+d, \tag{9}$$

where $\xi=Z_d^{0.8}Q_{2p}^{-1/2}$, with Z_d being the charge of the daughter nucleus. a, b, c and d are the fitting parameters, which are obtained by fitting the $2p$ decay half-lives estimated by the ELDM. These parameters are a = 0.1578, b = 1.9474, c = −1.8795, and d = −24.847, respectively. Liu's formula is written as [61]

$$\log_{10}T_{1/2}=a'(Z_d^{0.8}+l^{\beta})Q_{2p}^{-1/2}+b', \tag{10}$$

where the adjustable parameters a', b', and β, whose values are 2.032, −26.832, and 0.25, respectively, are obtained by fitting the experimental data and the calculated results based on the ELDM. Here β reflects the effect of the angular momentum on the $2p$ radioactivity half-lives.

Although the estimated ground state $2p$ decay half-lives within the UFM and the two formulas are in good agreement with the experimental values, their reliability needs to be tested with more experimental data. Some experimental $2p$ decay half-lives of the excited states have been accumulated in recent decades, which can be used for ground testing the validity of the UFM and the two formulas. Thus, the UFM and Eqs. (9, 10) are extended to study the excited states. In Table 3, the $2p$ transitions from the excited states to either the ground states or excited states are listed in column 1. The initial and final spin-parity values are given in column 2 and column 3, respectively. In columns 4-6, the l values, the Q_{2p} values, and the experimental logarithm half-lives are listed. The l values are extracted by the spin-parity selection rule and are selected to be zero for the cases of ^{22}Mg* and ^{29}S* because the spin-parity of their initial states has not been determined experimentally. As for ^{94}Ag*, the l value was conservatively estimated to be between 6 and 10$\hbar$ by assuming that the un-assigned γ-rays may take up to 4$\hbar$ of angular momentum [48]. Therefore, in our calculations, $l=6\sim10\hbar$ is used. Note that, in calculations, the S_{2p} values of the excited states are assumed to be the same as those of the ground states. The calculated logarithm half-lives within the UFM, Sreeja's formula, and Liu's for-

Table 2. Predicted $2p$ decay half-lives within the UFM, GLDM, and ELDM found by inputting the newest Q_{2p} values taken from the AME2020 table [94].

Nuclei	Q_{2p}/MeV	S_{2p}	l	$\log_{10} T^{2p}_{1/2}$/s		
				UFM	GLDM	ELDM
$^{5}_{4}$Be	7.63	0.053	0	−20.58	–	–
$^{6}_{5}$B	7.42	0.043	0	−20.41	–	–
$^{7}_{5}$B	1.42	0.037	0	−19.33	–	−19.19
$^{8}_{6}$C	2.11	0.045	0	−19.80	–	−19.26
$^{10}_{7}$N	1.30	0.035	1	−18.07	−17.98	−17.28
$^{11}_{8}$O	4.25	0.032	0	−19.67	–	−19.67
$^{13}_{9}$F	3.09	0.028	0	−19.33	–	−18.89
$^{14}_{9}$F	0.05	0.026	1	12.22	–	12.31
$^{15}_{10}$Ne	2.52	0.025	0	−18.57	−18.48	−18.08
$^{17}_{11}$Na	3.57	0.024	0	−18.95	–	−18.63
$^{22}_{14}$Si	1.58	0.021	0	−14.61	−18.87	−14.15
$^{24}_{15}$P	1.24	0.020	4	−8.50	−9.41	−8.44
$^{26}_{16}$S	2.36	0.019	0	−16.09	−19.64	−15.15
$^{28}_{17}$Cl	2.72	0.019	2	−15.29	−15.66	−14.47
$^{29}_{17}$Cl	0.10	0.018	0	28.91	–	29.44
$^{29}_{18}$Ar	5.90	0.018	0	−18.99	–	−18.35
$^{30}_{18}$Ar	3.42	0.018	0	−17.02	−19.66	−16.15
$^{31}_{19}$K	5.66	0.018	2	−18.21	−18.55	−17.29
$^{32}_{19}$K	2.74	0.017	2	−14.44	−14.78	−13.68
$^{33}_{20}$Ca	5.13	0.017	0	−18.11	−18.48	−17.35
$^{34}_{20}$Ca	2.51	0.017	0	−14.46	−14.78	−13.56
$^{35}_{21}$Sc	4.98	0.017	3	−16.10	−16.63	−15.57
$^{37}_{21}$Sc	0.38	0.017	3	10.92	10.10	10.97
$^{37}_{22}$Ti	5.40	0.017	0	−17.81	−17.96	−17.07
$^{38}_{22}$Ti	3.24	0.016	0	−15.18	−15.38	−14.30
$^{39}_{22}$Ti	1.06	0.016	0	−5.41	−5.55	−4.64
$^{39}_{23}$V	4.21	0.016	0	−16.34	−16.54	−15.49
$^{40}_{23}$V	2.14	0.016	0	−11.66	−11.80	−10.80
$^{41}_{24}$Cr	3.33	0.016	0	−14.53	−14.72	−13.66
$^{42}_{24}$Cr	1.48	0.016	0	−7.40	−7.56	−6.66
$^{43}_{25}$Mn	2.48	0.016	2	−10.65	−11.03	−10.16
$^{44}_{25}$Mn	0.50	0.016	0	9.80	9.51	10.22
$^{47}_{27}$Co	1.02	0.015	2	1.13	0.63	1.37
$^{49}_{28}$Ni	1.08	0.015	0	0.23	−0.08	0.67
$^{52}_{29}$Cu	1.13	0.015	4	3.45	2.70	3.34
$^{55}_{30}$Zn	0.78	0.015	2	8.77	8.26	8.92
$^{56}_{31}$Ga	2.82	0.014	0	−10.30	−10.83	−9.14
$^{57}_{31}$Ga	1.65	0.014	2	−3.01	−3.81	−2.20
$^{58}_{31}$Ga	0.51	0.014	2	18.71	17.88	19.33

Continued on next page

Table 2-continued from previous page

Nuclei	Q_{2p}/MeV	S_{2p}	l	$\log_{10} T^{2p}_{1/2}$/s		
				UFM	GLDM	ELDM
$^{58}_{32}$Ge	3.23	0.014	0	−11.19	−11.73	−10.02
$^{59}_{32}$Ge	1.60	0.014	0	−2.73	−3.37	−1.76
$^{60}_{33}$As	3.32	0.014	4	−8.37	−9.34	−7.81
$^{61}_{33}$As	1.98	0.014	0	−4.95	−5.61	−3.97
$^{62}_{33}$As	0.59	0.014	2	17.99	17.14	18.58
$^{63}_{34}$Se	2.36	0.013	0	−6.59	−7.22	−5.60
$^{64}_{34}$Se	0.70	0.013	0	14.39	13.69	15.14
$^{65}_{35}$Br	2.43	0.013	2	−5.55	−6.37	−4.76
$^{66}_{35}$Br	1.39	0.013	0	1.83	1.12	2.68
$^{68}_{36}$Kr	1.46	0.013	0	1.83	1.13	2.65
$^{81}_{42}$Mo	0.73	0.013	0	23.26	22.67	23.82
$^{85}_{44}$Ru	1.13	0.013	0	14.08	13.76	14.66
$^{108}_{54}$Xe	1.01	0.012	0	27.07	26.37	27.47

Table 3. Comparison between the experimental $2p$ radioactivity half-lives of the excited states and those within different models and formulas. The half-lives that are not available experimentally are also predicted. The symbol "*" represents the excited state of a nucleus.

Transitions	J^π_i	J^π_f	l	Q_{2p}/MeV	$\log_{10} T^{2p}_{1/2}$/s				
					Expt.	UFM	Sreeja	Liu	Other
$^{14}_{8}O^* \longrightarrow ^{12}_{6}C + 2p$	2^+	0^+	2	1.20[38]	>−16.12[38]	−16.02	−19.94	−16.85	−18.12[38]
	$(2)^+$	0^+	2	3.15[38]		−18.87	−23.26	−20.67	
	4^+	0^+	4	3.35[38]		−15.96	−26.46	−20.61	
$^{17}_{10}Ne^* \longrightarrow ^{15}_{8}O + 2p$	$3/2^-$	$1/2^-$	2	0.35[39,40]	>−10.59[40]	−7.11	−8.42	−4.62	−9.40[11]
	$3/2^-$	$1/2^-$	2	0.35[39,40]					−6.89[52]
	$3/2^-$	$1/2^-$	2	0.35[39,40]					$-6.33^{+0.09}_{-0.10}$[64]
	$5/2^-$	$1/2^-$	2	0.82[39,40]		−12.73	−15.42	−12.32	
	$1/2^+$	$1/2^-$	1	0.97[39,40]		−14.69	−15.44	−13.88	
$^{18}_{10}Ne^* \longrightarrow ^{16}_{8}O + 2p$	2^+	0^+	2	0.59[42]		−10.91	−13.06	−9.72	
	1^-	0^+	1	1.63[42]	$-16.15^{+0.06}_{-0.06}$[42,43]	−16.79	−18.02	−16.84	−17.12[42]
$^{22}_{12}Mg^* \longrightarrow ^{20}_{10}Ne + 2p$	–	0^+	0	6.11[44,45]		−18.97	−19.88	−21.65	
$^{29}_{16}S^* \longrightarrow ^{27}_{14}Si + 2p$	–	$5/2^+$	0	1.72~2.52[46]		−16.4~−14.3	−14.7~−12.6	−16.3~−14.0	
	–	$5/2^+$	0	4.32~5.12[46]		−18.9~−18.5	−17.7~−17.1	−19.4~−18.8	
$^{94}_{47}Ag^* \longrightarrow ^{92}_{45}Rh^* + 2p$	21^+	11^+	6~10	1.90[48]	$1.90^{+0.38}_{-0.20}$[48]	9.38~15.21	8.00~10.10	6.46~6.77	4.70[57]
				1.98[105]		8.56~14.37	7.10~9.01	5.78~6.09	
				2.05[105]		7.89~13.68	6.36~8.11	5.22~5.52	
				3.45[105]		−0.92~4.56	−3.75~−3.38	−-2.13~−1.89	

mula are listed in columns 7-9. In addition, the half-lives extracted from other models are listed in the final column.

In the next paragraphs, $2p$ radioactivity of the excited states will be discussed by analyzing the calculated results in Table 3. For $^{14}O^*$, a weak $2p$ decay branch with $\Gamma = 125 \pm 20$ eV via the 2^+ state ($E^* = 7.77$ MeV, E^* is the excitation energy) was observed which occurs predominantly by a sequential mechanism [38]. However, an upper limit of the ^{2}He emission $\Gamma_{^2\mathrm{He}} < 6$ eV was measured

[38], which corresponds to $\log_{10}T_{1/2}^{2p}>-16.12$ s. By comparing the measured half-life with those estimated by the UFM, Sreeja's formula, Liu's formula, and *R*-matrix theory [38], it is shown that only the half-life within the UFM is larger than the experimental lower limit. For ^{17}Ne*, the $2p$ decays from its first two excited states ($3/2^-$ and $5/2^-$ states) were studied using intermediate energy Coulomb excitation combined with $2p$ spectroscopy [40] and a previously performed γ spectroscopy experiment [39]. It was found that the $5/2^-$ state (E^* = 1.764 MeV) decays, via the sequential $2p$ emission, to the ground state of ^{15}O. However, no evidence of a simultaneous $2p$ decay from the first excited $3/2^-$ state was observed. A lifetime limit $\tau_{2p} > 26$ ps ($\log_{10}T_{1/2}^{2p}>-10.59$ s) of the $3/2^-$ state (E^* = 1.288 MeV) was obtained. As seen in Table 3, the $2p$ decay half-lives of ^{17}Ne* within all the models are in agreement with the corresponding measured half-life. As for ^{18}Ne*, clear evidence of the simultaneous $2p$ emission from the 1^- state (E^* = 6.15 MeV) was observed with the reaction ^{17}F+^{1}H [42]. However, the two extreme decay mechanisms (the ^{2}He emission and direct three-body decay with no final state interactions) were not distinguished by the measured data due to the limited angular coverage. Nevertheless, the $2p$ partial width Γ_{2p} was found to be 21 ± 3 eV, when assuming ^{2}He emission, and 57 ± 6 eV, when assuming three-body decay. Subsequently, new experimental evidence for ^{2}He emission from the ^{18}Ne excited states was observed by a complete kinematical reconstruction of the decay products at the in-Flight Radioactive Ion Beams (FRIBs) facility of the Laboratori Nazionali del Sud (LNS)-Italy [43]. It was found that the 1^- state $2p$ decay proceeds through ^{2}He diproton resonance (31%) and democratic or virtual sequential decay (69%). By combining the measurements of Gómez del Campo *et al.* [42] and Raciti *et al.* [43], it is evident that the real experimental $\Gamma_{^2\mathrm{He}}$ of the 1^- state of ^{18}Ne is 6.51 ± 0.93 eV, corresponding to a logarithm lifetime of -16.15 ± 0.06 s. By comparing the experimental half-life with the estimated values from the four approaches ($\log_{10}T_{1/2}^{2p}$ = –17.12 s is estimated from a simple *R*-matrix [42]), the half-life extracted from the UFM is closest to the experimental value.

In recent years, measurements of the decay properties of the 21^+ high-spin isomer in ^{94}Ag have been performed because its properties are unique within the entire nuclear chart. This isomer state with a high excitation energy of 6.7(5) MeV and a long half-life of 0.39(4) s makes several decay modes possible: a β decay followed by a γ-ray or proton emission [101, 102], a β-delayed γ, $1p$ and $2p$ decays [101-104], direct $1p$ and $2p$ emissions [48, 105-108], and α-radioactivity [109]. The β-delayed γ, $1p$, and $2p$ decays from the 21^+ isomer have been reported in [101-104], and then, experiments on direct $1p$ and $2p$ emissions of the 21^+ isomer were performed in several labs [48, 105-108]. In 2005, direct $1p$ decay of the 21^+ isomer into two high-spin daughter states in ^{93}Pd was identified by detecting protons in coincidence with γ-γ correlations and applying γ gates based on known ^{93}Pd levels [106]. A strong quenching of the partial decay width indicates the importance of parent state deformation. One year later, evidence of the simultaneous $2p$ emission of the 21^+ isomer to an excited state of the daughter nucleus ^{92}Rh was reported [48]. The $2p$ branch was characterized by Q_{2p} = 1.9(1) MeV and a decay probability of 0.5(3)% leading to $T_{1/2}^{2p}$ = 80 s; the $2p$ decay behavior and the unexpectedly large probability were explained by assuming a strong prolate deformation of the 21^+ isomer. However, the possibility of $2p$ decay of the 21^+ isomer was questioned by a measurement by Pechenaya *et al.* [107]. To uncover the nature of this isomer and its possible decay modes, the masses of ^{93}Pd and ^{94}Ag were deduced by measuring the masses of the $2p$ decay daughter ^{92}Rh and the β-decay daughter ^{94}Pd of the high-spin isomer in ^{94}Ag with the Penning trap mass spectrometer JYFLTRAP at the Ion-Guide Isotope Separator On-Line [105]. It was found that the E^* value of the 21^+ isomer is 6.96 (8.36) MeV, when combined with data from the $1p$ ($2p$) decay experiments. This indicates that the E^* value of the 21^+ isomer has been uncertain. However, using the two different E^* values and the AME2003 data, the extracted Q_{2p} values of this isomeric state are 2.05, 3.45, and 1.98 MeV [105]. The corresponding half-lives from the UFM and the formulas of Sreeja and Liu, found by inputting the three Q_{2p} values and the Q_{2p} value in Ref. [48], are listed in the final four lines of Table 3. In calculations, the l values are taken as $6\sim10\hbar$ as done in the model in Ref. [48]. From Table 3, it is seen that the experimental half-life is reproduced only in the UFM by inputting Q_{2p} = 3.45 MeV. According to the above discussion on $2p$ decay of the excited states of ^{14}O, ^{17}Ne, ^{18}Ne, and ^{94}Ag, it is shown that the predictive power of the UFM is stronger than that of the formulas of Sreeja and Liu because more nuclear structure details are included in it. Therefore, the half-lives that are not available experimentally but predicted by the UFM (see Table 3) appear to be more reliable. However, a reinvestigation by Cerny *et al.* in 2009 found no evidence to support $2p$ radioactivity of the long-lived isomer in ^{94}Ag* [108]. Due to these contradictory measurements [48, 105, 107, 108] and the argument between Mukha and Pechenaya [110, 111], it remains a mystery whether $2p$ radioactivity exists in the long-lived isomer of ^{94}Ag*. We fully agree with the viewpoint of Ref. [105]: to finally solve this puzzle, direct mass measurements of ^{93}Pd, ^{94}Ag, and ^{94}Ag* (21^+) are needed, posing new challenges for the production of these exotic species. The direct mass measurements of these exotic nuclei are expected with the new generation of radioactive beam facilities [112-114].

In addition, $2p$ emission was observed from the higher excited states of ^{17}Ne [41] and ^{18}Ne [43]. In ^{17}Ne, a correlated $2p$ emission via ^{2}He resonance might be observed from one or several states with an excitation energy above 2 MeV [41]. The $2p$ decay of the high-lying states in ^{18}Ne seems to occur predominantly via a democratic or true sequential decay mechanism [43]. However, the two hypotheses have not yet been tested with further experiments. ^{17,18}Ne beams with high intensities can be applied at new radioactive beam facilities, such as the High Intensity heavy-ion Accelerator Facility (HIAF) of China [112], to test these hypotheses in the future. In contrast, it is recommended that some microscopic models, for example, the shell model, should be developed by taking into account necessary physical factors, such as the tensor force [115], three-body force [116], and accurate pairing force [117], to reasonably describe the mechanism of $2p$ emission from the excited states.

It is well known that the $2p$ decay half-life is sensitive to the Q_{2p} and l values [57-61, 89]. Because the Q_{2p} and/or l values of the $2p$ decay of ^{22}Mg*, ^{29}S*, and ^{94}Ag* are uncertain, the $2p$ decay half-lives of the excited states for the three nuclei versus l, which are obtained by inputting different Q_{2p} values, are plotted in Figs. 1-3. Fig. 1 shows that the $\log_{10}T_{1/2}^{2p}$ curves are very different from one another. For the $2p$ decay of ^{22}Mg*, Z_d = 10 and Q_{2p} = 6.11 MeV, and the specific forms of Sreeja's formula and Liu's formula are $\log_{10}T_{1/2}(\text{Sreeja}) = -1.477l - 19.875$ and $\log_{10}T_{1/2}(\text{Liu}) = -21.639 + 0.823l^{0.25}$, respectively. Thus, the relation between $\log_{10}T_{1/2}^{2p}$ and l is linear for Sreeja's formula and non-linear (a power function) for Liu's formula. In the framework of the UFM, the quantity $\log_{10}T_{1/2}(l>0)$ can be written as [78, 79]

$$\log_{10}T_{1/2}(l>0) = \log_{10}T_{1/2}(l=0) + c\frac{l(l+1)}{\sqrt{\mu Z_1 Z_2 R_{in}}}, \quad (11)$$

where $\log_{10}T_{1/2}(l=0)$ represents the logarithm half-life for the vanishing l, and c is a constant. According to Eq. (11), the relation between $\log_{10}T_{1/2}(l>0)$ and l is described by a parabolic curve. Similar tendencies can be obtained from the three methods as shown in Figs. 2 and 3. In addition, as shown in Fig. 2(b), the half-lives decrease with the increase in l. For the case of ^{94}Ag*, only the calculated half-lives based on the UFM, with Q_{2p} = 3.45 MeV, are in agreement with the experimental data, as previously discussed during the analysis of Table 3. However, for the formula of Sreeja, the half-lives decrease with l in the case of Q_{2p} = 3.45 MeV, and the evolution trend is the same as that of Fig. 2(b); this is unreasonable because, if l increases, the half-life becomes

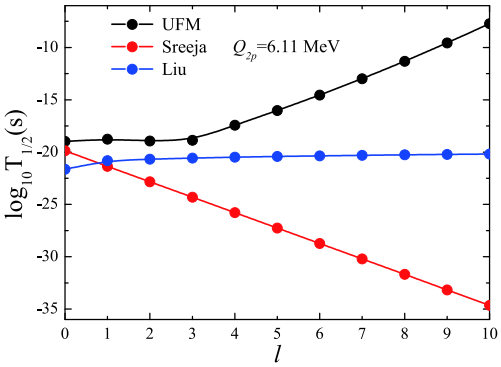

Fig. 1. (color online) $2p$ radioactivity half-lives of ^{22}Mg* within the UFM and the formulas of Sreeja and Liu as functions of l.

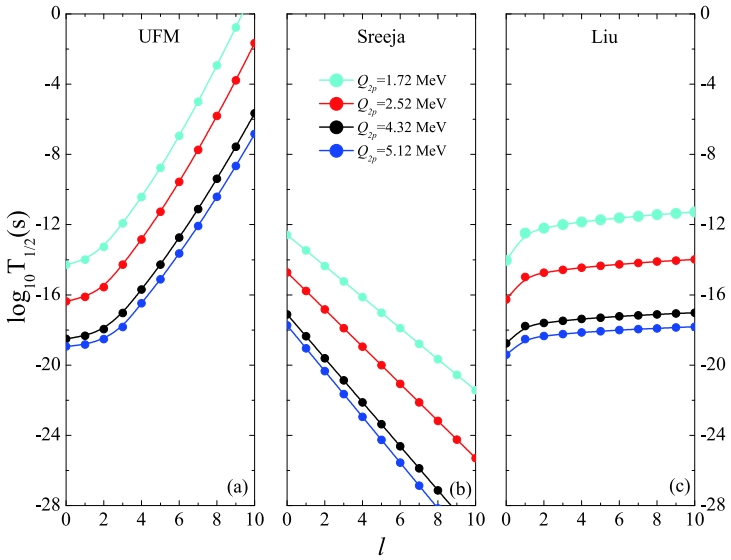

Fig. 2. (color online) $2p$ radioactivity half-lives of ^{29}S* within the UFM and the formulas of Sreeja and Liu by inputting different Q_{2p} values as functions of l.

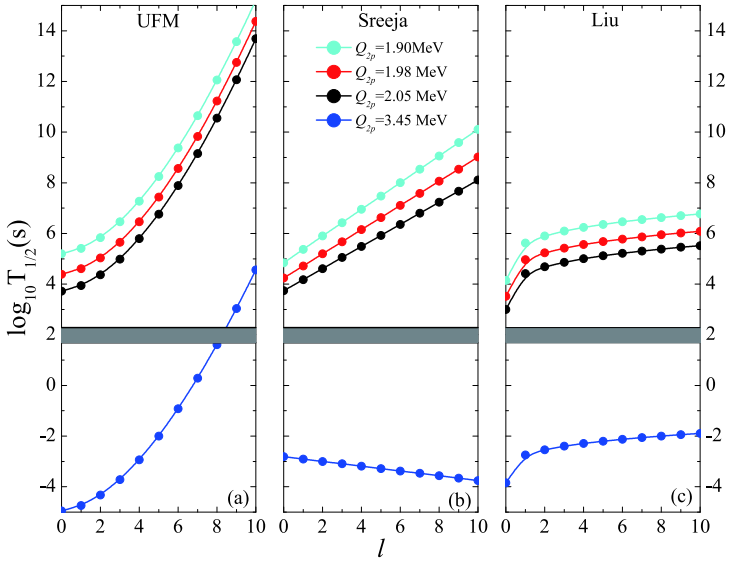

Fig. 3. (color online) Same as Fig. 2, but for the case of ^{94}Ag*. The shaded area represents its experimental half-life.

longer with the increase in the centrifugal barrier. For Liu's formula, although the half-life increases as l increases, this increase is abnormally slow, which can be seen from Figs. 2(c) and 3(c). However, relevant studies indicate that the half-life is clearly enhanced by a large l value, for example, in the case of α decay [118]. Hence, the two fitting formulas are not suitable for the study of $2p$ radioactivity of the excited states. This conclusion is further reinforced by the following. (i) The parameters involved in the two formulas are obtained by fitting a small number of ground state experimental data and/or ground state half-lives within the ELDM by inputting the Q_{2p} values extracted from the AME2016 table [86]. By comparing the AME2016 table [86] and AME2020 table [94], the two types of Q_{2p} values are found to be very different. This leads to a large difference in the half-lives estimated within the ELDM by inputting the two types of Q_{2p} values because the half-lives are sensitive to the Q_{2p} values, which can be seen through a comparison of Table 2 from this article and Table 2 from Ref. [58]. (ii) The experimental data from the excited states are not included in the fitting procedure. If the Q_{2p} values of the AME2020 table are more reliable than those of the AME2016 table, the universal parameters can be obtained by fitting the experimental half-lives of the ground and excited states and the predicted ground state half-lives, within a plausible model, by inputting the Q_{2p} values taken from the AME2020 table. In summary, more nuclear structure information can be obtained by investigating $2p$ radioactivity of excited states, which is difficult to observe but worth studying further.

IV. CONCLUSIONS

In this study, the UFM was firstly extended to study the $2p$ radioactivity half-lives of the ground states of nuclei by introducing the parametric spectroscopic factor. The probable $2p$ radioactivity candidates of the ground states were predicted within the UFM by inputting the Q_{2p} values from the AME2020 table. Finally, $2p$ radioactivity of the excited states of ^{14}O, ^{17,18}Ne, ^{22}Mg, ^{29}S, and ^{94}Ag was discussed using the UFM, Sreeja's formula, and Liu's formula. The obtained results allow us to draw the following conclusions:

(i) The calculated half-lives of ground states within the UFM are in good agreement with the experimental values.

(ii) Because the UFM has a similar physical mechanism to the GLDM, ELDM, and Gamow-like model, the predicted half-lives of the ground states within the four models are similar. Furthermore, using the extended half-life constraint condition, the most probable $2p$ decay candidates predicted by the UFM, GLDM, and ELDM are ^{24}P, ^{39}Ti, ^{40}V, ^{42}Cr, ^{43}Mn, ^{47}Co, ^{49}Ni, ^{56,57}Ga, ^{58,59}Ge, ^{60,61}As, ^{63}Se, ^{65,66}Br, and ^{68}Kr.

(iii) The experimental $2p$ radioactivity half-lives of the excited states of ^{14}O, ^{17,18}Ne, and ^{94}Ag are reproduced better by the UFM than the formulas of Sreeja and Liu because the former includes more details of nuclear structure. Therefore, the $2p$ radioactivity half-lives of the excited states that are not available experimentally but predicted by the UFM are more plausible.

(iv) Sreeja's formula and Liu's formula are not suitable for investigating $2p$ radioactivity of the excited states. First, they contradict the fact that the half-life increases as the angular momentum increases. Second, the

parameters of the two formulas are obtained only by fitting the 2p decay data of the ground states and contain no information about the excited states. Thus, to propose a universal formula that estimates the 2p decay half-lives of both the ground and excited states, more 2p decay data of ground and excited states should be used in the fitting procedure, which are expected to be measured in a new generation of radioactive beam facilities.

V. ACKNOWLEDGEMENTS

We thank professor Shangui Zhou, professor Ning Wang, professor Fengshou Zhang, and Dr. Yang Xiao for helpful discussions.

References

[1] Y. B. Zel'dovich, Sov. Phys.-JETP **11**, 812 (1960)
[2] V. I. Goldansky, Nucl. Phys. **19**, 482 (1960)
[3] V. I. Goldansky, Nucl. Phys. **27**, 648 (1961)
[4] M. Pfützner, M. Karny, L. Grigorenko *et al.*, Rev. Mod. Phys. **84**, 567 (2012)
[5] B. Blank and M. Ploszajczak, Rep. Prog. Phys. **71**, 046301 (2008)
[6] B. Blank and M. J. G. Borge, Prog. Part. Nucl. Phys. **60**, 403 (2008)
[7] V. I. Goldanskii, Nuovo Cimento **25**(Suppl. 2), 123 (1962)
[8] V. I. Goldanskii, Phys. Lett. **14**, 233 (1965)
[9] V. I. Goldanskii , Sov. Phys.—Usp. **8**, 770 (1966)
[10] J. Jänecke, Nucl. Phys. **61**, 326 (1965)
[11] B. A. Brown, Phys. Rev. C **43**, R1513 (1991)
[12] B. J. Cole, Phys. Rev. C **54**, 1240 (1996)
[13] W. E. Ormand, Phys. Rev. C **53**, 214 (1996)
[14] M. Pfützner, E. Badura, C. Bingham *et al.*, Eur. Phys. J. A **14**, 279 (2002)
[15] J. Giovinazzo, B. Blank, M. Chartier *et al.*, Phys. Rev. Lett. **89**, 102501 (2002)
[16] B. Blank, A. Bey, G. Canchel *et al.*, Phys. Rev. Lett. **94**, 232501 (2005)
[17] C. Dossat, A. Bey, B. Blank *et al.*, Phys. Rev. C **72**, 054315 (2005)
[18] T. Goigoux, P. Ascher, B. Blank *et al.*, Phys. Rev. Lett. **117**, 162501 (2016)
[19] W. Whaling, Phys. Rev. C **150**, 836 (1966)
[20] M. F. Jager, R. J. Charity, J. M. Elson *et al.*, Phys. Rev. C **86**, 011304 (2012)
[21] G. J. KeKelis, M. S. Zisman, D. K. Scott *et al.*, Phys. Rev. C **17**, 1929 (1978)
[22] R. A. Kryger *et al.*, Phys. Rev. Lett. **74**, 860 (1995)
[23] D. Suzuki *et al.*, Phys. Rev. Lett. **103**, 152503 (2009)
[24] C. J. Woodward, R. E. Tribble, D. M. Tanner *et al.*, Phys. Rev. C **27**, 27 (1983)
[25] I. Mukha, K. Sümmerer, L. Acosta *et al.*, Phys. Rev. Lett. **99**, 182501 (2007)
[26] O. V. Bochkarev *et al.*, Nucl. Phys. A **505**, 215 (1989)
[27] V. I. Goldansky, JETP Lett. **39**, 554 (1980)
[28] M. D. Cable, J. Honkanen, R. F. Parry *et al.*, Phys. Rev. Lett. **50**, 404 (1983)
[29] B. Blank, F. Boué, S. Andriamonje *et al.*, Z. Phys. A **357**, 247 (1997)
[30] J. Honkanen, M. D. Cable, R. F. Parry *et al.*, Phys. Lett. B **133**, 146 (1983)
[31] V. Borrel *et al.*, Nucl. Phys. A **473**, 331 (1987)
[32] J. E. Reiff, M. A. C. Hotchkis, D. M. Moltz *et al.*, Nucl. Instrum. Methods A **276**, 228 (1989)
[33] J. Äystö, D. M. Moltz, X. J. Xu *et al.*, Phys. Rev. Lett. **55**, 1384 (1985)
[34] D. M. Moltz, J. C. Batchelder, T. F. Lang *et al.*, Z. Phys. A **342**, 273 (1992)
[35] V. Borrel, R. Anne, D. Bazin *et al.*, Z. Phys. A **344**, 135 (1992)
[36] J. Giovinazzo *et al.*, Phys. Rev. Lett. **99**, 102501 (2007)
[37] C. Dossat, N. Adimi, F. Aksouh *et al.*, Nucl. Phys. A **792**, 18 (2007)
[38] C. R. Bain, P. J. Woods, R. Coszach *et al.*, Phys. Lett. B **373**, 35 (1996)
[39] M. Chromik, B. A. Brown, M. Fauerbach *et al.*, Phys. Rev. C **55**, 1676 (1997)
[40] M. J. Chromik, P. G. Thirolf, M. Thoennessen *et al.*, Phys. Rev. C **66**, 024313 (2002)
[41] T. Zerguerras, B. Blank, Y. Blumenfeld *et al.*, Eur. Phys. J. A **20**, 389 (2004)
[42] J. Gómez del Campo, A. Galindo-Uribarri, J. R. Beene *et al.*, Phys. Rev. Lett. **86**, 43 (2001)
[43] G. Raciti, G. Cardella, M. De Napoli *et al.*, Phys. Rev. Lett. **100**, 192503 (2008)
[44] Y. G. Ma, D. Q. Fang, X. Y. Sun *et al.*, Phys. Lett. B **743**, 306 (2015)
[45] D. Q. Fang, Y. G. Ma, X. Y. Sun *et al.*, Phys. Rev. C **94**, 044621 (2016)
[46] C. J. Lin, X. X. Xu, H. M. Jia *et al.*, Phys. Rev. C **80**, 014310 (2009)
[47] X. X. Xu, C. J. Lin, H. M. Jia *et al.*, Phys. Lett. B **727**, 126 (2013)
[48] I. Mukha, E. Roeckl, L. Batist *et al.*, Nature **439**, 298 (2006)
[49] V. M. Galitsky and V. F. Cheltsov, Nucl. Phys. **56**, 86 (1964)
[50] W. Nazarewicz, J. Dobaczewski, T. R. Werner *et al.*, Phys. Rev. C **53**, 740 (1996)
[51] W. E. Ormand, Phys. Rev. C **55**, 2407 (1997)
[52] F. C. Barker, Phys. Rev. C **63**, 047303 (2001)
[53] B. A. Brown and F. C. Barker, Phys. Rev. C **67**, 041304 (2003)
[54] L. V. Grigorenko and M. V. Zhukov, Phys. Rev. C **76**, 014008 (2007)
[55] D. S. Delion, R. J. Liotta, and R. Wyss, Phys. Rev. C **87**, 034328 (2013)
[56] J. Rotureau, J. Okolowicz, and M. Ploszajczak, Nucl. Phys. A **767**, 13 (2006)
[57] J. P. Cui, Y. H. Gao, Y. Z. Wang *et al.*, Phys. Rev. C **101**, 014301 (2020)
[58] M. Gonalves, N. Teruya, and O. Tavares *et al.*, Phys. Lett. B **774**, 14 (2017)
[59] H. M. Liu, X. Pan, Y. T. Zou *et al.*, Chin. Phys. C **45**, 044110 (2021)
[60] I. Sreeja and M. Balasubramaniam, Eur. Phys. J. A **55**, 33 (2019)
[61] H. M. Liu, Y. T. Zou, X. Pan *et al.*, Chin. Phys. C **45**,

024108 (2021)
[62] E. Olsen, M. Pfützner, N. Birge *et al*., Phys. Rev. Lett. **110**, 222501 (2013); **111**, 139903 (2013)
[63] B. V Danilin and M. V. Zhukov, Phys. At. Nucl. **56**, 460 (1993)
[64] L. V. Grigorenko, R. C. Johnson, I. G. Mukha *et al*., Phys. Rev. Lett. **85**, 22 (2000)
[65] V. Vasilevsky, A. Nesterov, F. Arickx *et al*., Phys. Rev. C **63**, 034607 (2001)
[66] L. V. Grigorenko, I. G. Mukha, I. J. Thompson *et al*., Phys. Rev. Lett. **88**, 042502 (2002)
[67] L. V. Grigorenko and M. V. Zhukov, Phys. Rev. C **68**, 054005 (2003)
[68] P. Descouvemont, E. Tursunov, and D. Baye, Nucl. Phys. A **765**, 370 (2006)
[69] L. V. Grigorenko, R. C. Johnson, I. G. Mukha *et al*., Phys. Rev. C **64**, 054002 (2001)
[70] E. Garrido, A. Jensen, and D. Fedorov, Phys. Rev. C **78**, 034004 (2008)
[71] R. Álvarez-Rodríguez, A. S. Jensen, E. Garrido *et al*., Phys. Rev. C **77**, 064305 (2008)
[72] R. Álvarez-Rodríguez, A. S. Jensen, E. Garrido *et al*., Phys. Rev. C **82**, 034001 (2010)
[73] B. Blank, P. Ascher, L. Audirac *et al*., Acta Phys. Pol. B **42**, 545 (2011)
[74] J. L. Fisker, F. K. Thielmann, and M. Wiescher, Astrophys. J. **608**, L61 (2004)
[75] S. S. Malik and R. K. Gupta, Phys. Rev. C **39**, 1992 (1989)
[76] M. Balasubramaniam and R. K. Gupta, Phys. Rev. C **60**, 064316 (1999)
[77] M. Balasubramaniam and N. Arunachalam, Phys. Rev. C **71**, 014603 (2005)
[78] J. M. Dong, H. F. Zhang, J. Q. Li *et al*., Eur. Phys. J. A **41**, 197 (2009)
[79] J. M. Dong, H. F. Zhang, W. Zuo *et al*., Chin. Phys. C **34**, 182 (2010)
[80] T. B. Zhu, B. T. Hu, H. F. Zhang *et al*., Commun. Theor. Phys. **55**, 307 (2011)
[81] K. P. Santhosh and R. K. Biju, J. Phys. G: Nucl. Part. Phys. **36**, 015107 (2009)
[82] N. Anyas-Weiss, J. C. Cornell, P. S. Fisher *et al*., Phys. Rep. **12**, 201 (1974)
[83] A. Bohr and B. R. Mottelson, *Nuclear Structure* (W. A. Benjamin, New York, 1969), Vol. 1.
[84] L. Audirac, P. Ascher, B. Blank *et al*., Eur. Phys. J. A **48**, 179 (2012)
[85] M. Pomorski, M. Pfützner, W. Dominik *et al*., Phys. Rev. C **90**, 014311 (2014)
[86] M. Wang, G. Audi, F. G. Kondev *et al*., Chin. Phys. C **41**, 030003 (2017)
[87] M. Pomorski, M. Pfützner, W. Dominik *et al*., Phys. Rev. C **83**, 061303(R) (2011)
[88] P. Ascher, L. Audirac, N. Adimi *et al*., Phys. Rev. Lett. **107**, 102502 (2011)
[89] Y. Z. Wang, J. P. Cui, Y. H. Gao *et al*., Commun. Theor. Phys. **73**, 075301 (2021)
[90] N. Wang, M. Liu, X. Z. Wu *et al*. http://www.imqmd.com/mass/
[91] P. Möller, A. J. Sierk, T. Ichikawa *et al*., At. Data Nucl. Data Tables **109-110**, 1 (2016); P. Möller, M. R. Mumpower, T. Kawano *et al*., At. Data Nucl. Data Tables **125**, 1 (2019)
[92] H. Koura, T. Tachibana, and M. Uno, Prog. Theor. Phys. **113**, 305 (2005)
[93] S. Goriely, Nucl. Phys. A **933**, 68 (2014); http://www-astro.ulb.ac.be/bruslib/nucdata
[94] M. Wang, W. J. Huang, F. G. Kondev *et al*., Chin. Phys. C **45**, 030003 (2021)
[95] F. G. Kondev, M. Wang, W. J. Huang *et al*., Chin. Phys. C **45**, 030001 (2021)
[96] Y. Z. Wang, S. J. Wang, Z. Y. Hou *et al*., Phys. Rev. C **92**, 064301 (2015)
[97] Y. H. Gao, J. P. Cui, Y. Z. Wang *et al*., Sci. Rep. **10**, 9119 (2020)
[98] Y. Z. Wang, F. Z. Xing, Y. Xiao *et al*., Chin. Phys. C **45**, 044111 (2021)
[99] Y. Z. Wang, J. P. Cui, Y. L. Zhang *et al*., Phys. Rev. C **95**, 014302 (2017)
[100] Y. Z. Wang, Y. H. Gao, J. P. Cui *et al*., Commun. Theor. Phys. **72**, 025303 (2020)
[101] C. Plettner *et al*., Nucl. Phys. A **733**, 20 (2004)
[102] I. Mukha *et al*., Nucl. Phys. A **746**, 66c (2004)
[103] M. La Commara *et al*., Nucl. Phys. A **708**, 167 (2002)
[104] I. Mukha *et al*., Phys. Rev. C **70**, 044311 (2004)
[105] A. Kankainen, V.-V. Elomaa, L. Batist *et al*., Phys. Rev. Lett. **101**, 142503 (2008)
[106] I. Mukha, E. Roeckl, J. Döring *et al*., Phys. Rev. Lett. **95**, 022501 (2005)
[107] O. L. Pechenaya, C. J. Chiara, D. G. Sarantites *et al*., Phys. Rev. C **76**, 011304(R) (2007)
[108] J. Cerny, D. M. Moltz, D. W. Lee *et al*., Phys. Rev. Lett. **103**, 152502 (2009)
[109] G. Audi, A. H. Wapstra, and C. Thibault, Nucl. Phys. A **729**, 337 (2003)
[110] I. Mukha, H. Grawe, E. Roeckl *et al*., Phys. Rev. C **78**, 039803 (2008)
[111] O. L. Pechenaya, D. G. Sarantites, W. Reviol *et al*., Phys. Rev. C **78**, 039804 (2008)
[112] Y. G. Ma and H. W. Zhao, Sci. Sin.-Phys. Mech. Astron. **50**, 112001 (2020)
[113] M. S. Avilov, L. B. Tecchio, A. T. Titov *et al*., Nucl. Instr. Meth. A **618**, 1 (2010)
[114] Y. Yano, Nucl. Instr. Meth. Phys. Res. B **261**, 1009 (2007)
[115] T. Otsuka, T. Suzuki, R. Fujimoto *et al*., Phys. Rev. Lett. **95**, 232502 (2005)
[116] J. D. Holt, J. Menéndez, and A. Schwenk, Phys. Rev. Lett. **110**, 022502 (2013)
[117] C. Qi and T. Chen, Phys. Rev. C **92**, 051304 (2015)
[118] J. M. Dong, H. F. Zhang, Y. Z. Wang *et al*., Nucl. Phys. A **832**, 198 (2010)